Electronic Supplementary Material (ESI) for Sustainable Energy & Fuels.

Supporting Information

Synthesis of flower-like nickel-iron-chromium nanostructure compound deposited stainless steel foil as efficient binder-free electrocatalysts for water splitting

Caixia Zhou, [*a] *Taotao Gao,* [b] *Jiong Tan,* [a] *Zhaozu Luo,* [a] *Lutfy Mutallip,* [a] *and Dan Xiao* [*b]

[a] C. Zhou, J. Tan, Z Luo, L. Mutallip

College of Chemistry & Environment

Southwest Minzu University

Chengdu 610041, PR China

E-mail: cx_Zhou123@163.com

[b] T. Gao, Prof. D. Xiao

College of Chemical Engineering

Sichuan University

Chengdu, 610065, P. R. China

E-mail: xiaodan@scu.edu.cn

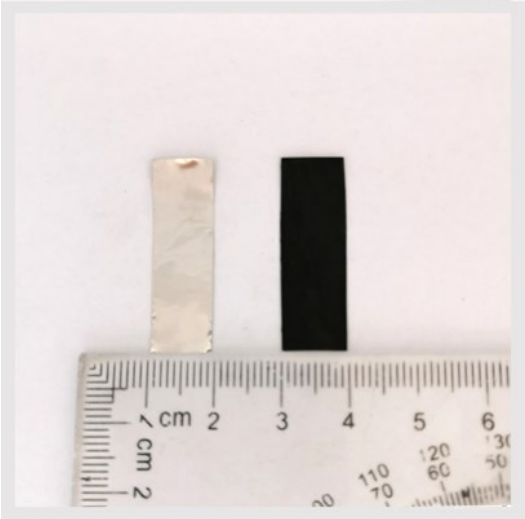

Fig. S1 The photograph of blank SSF substrate and NICC/SSF electrode.

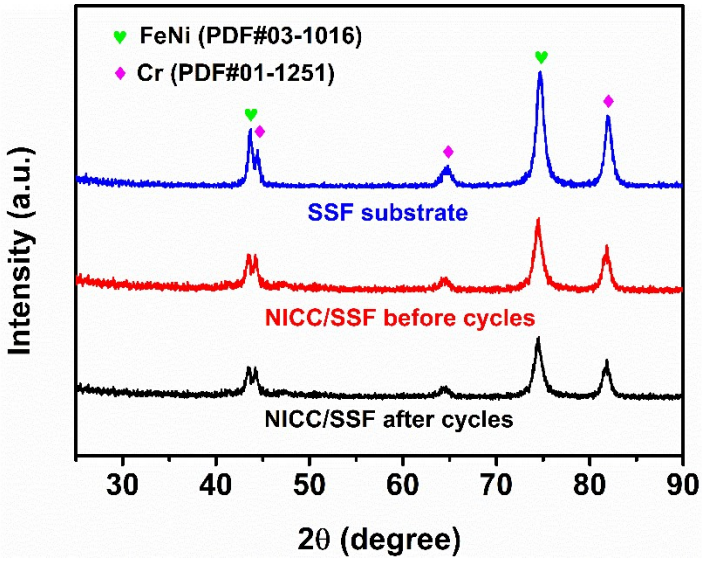

Fig. S2 The XRD patterns of SSF substrate and NICC/SSF samples before and after cycles.

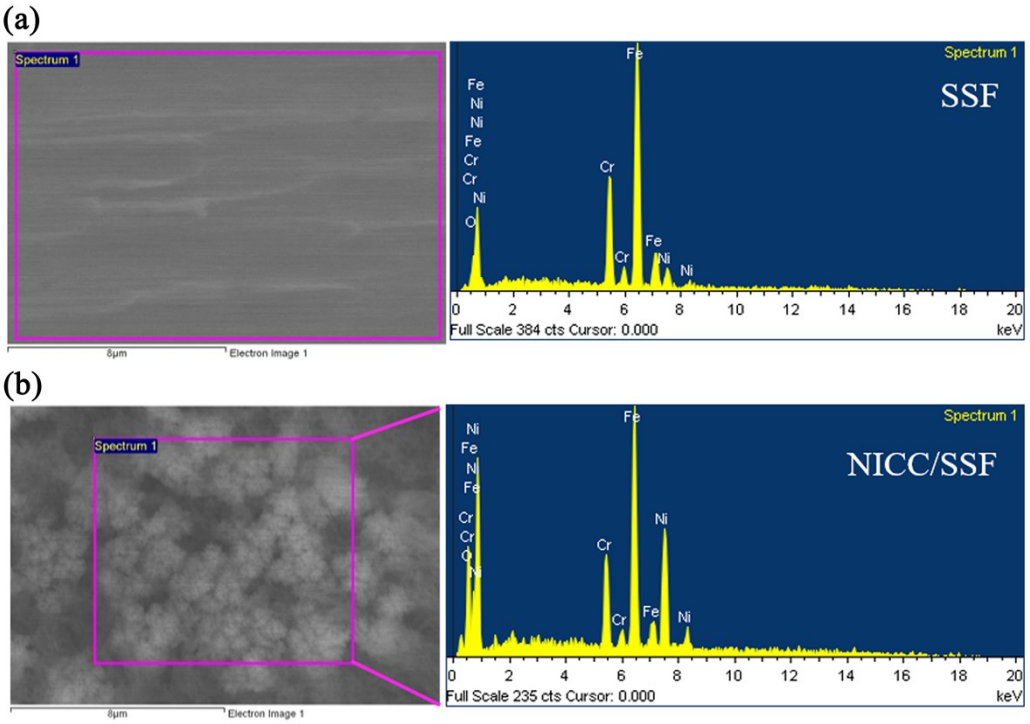

Fig. S3 EDX spectra of the SSF substrate (a) and NICC/SSF (b) after electrodeposition.

Table S1. The element distribution on the surface of SSF (stainless steel film) and NICC/SSF determined from XPS.

NICC/SSF	
Element	**Weight Conc.%**
Ni	33.99
Fe	41.25
Cr	11.61
O	13.15

SSF	
Element	**Weight Conc.%**
Ni	7.96
Fe	71.96
Cr	19.37
O	0.71

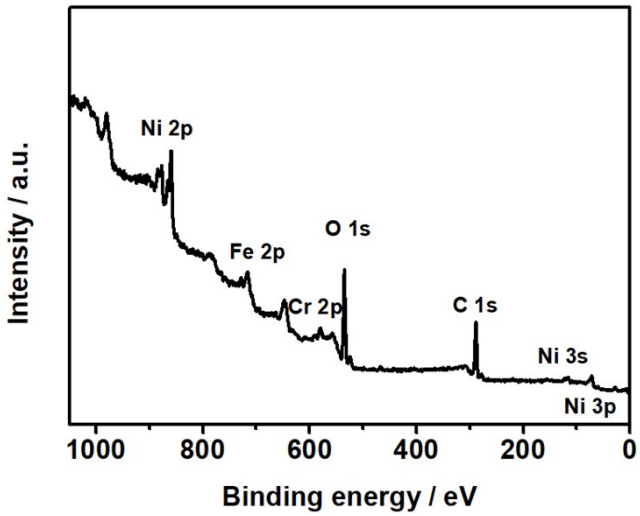

Fig. S4 The Full-scan XPS spectrum of NICC/SSF sample.

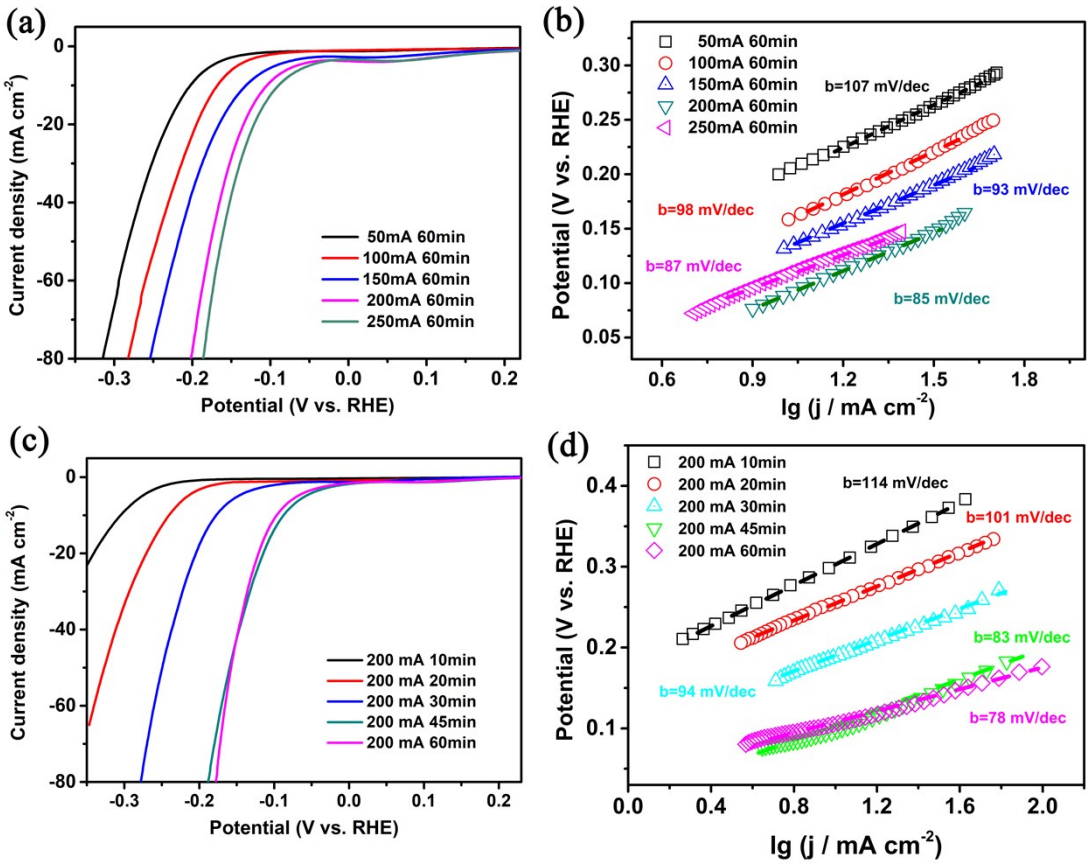

Fig. S5 (a and b) The LSV curves and Tafel plots of NICC/SSF samples at various deposition current; (c and d) The LSV curves and Tafel plots of NICC/SSF samples at different deposition time.

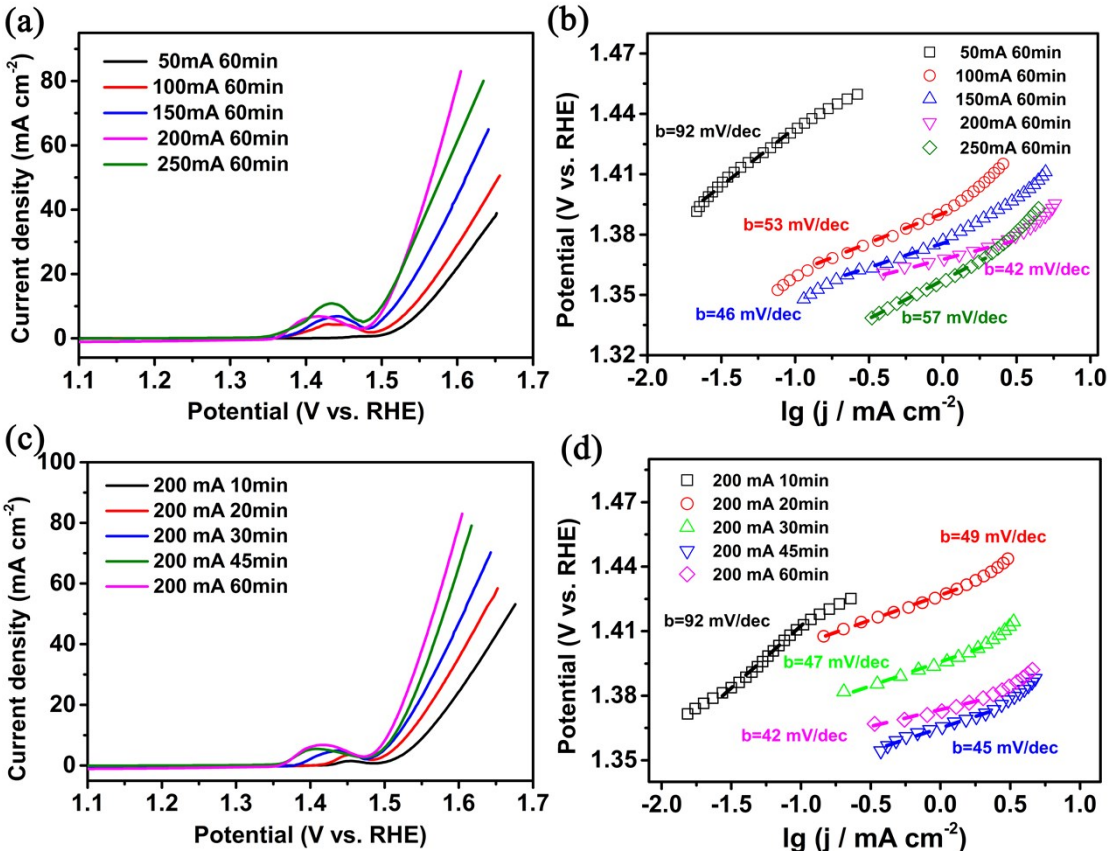

Fig. S6 (a) the polarization curves and (b) the corresponding Tafel plots of NICC/SSF electrodes at various electrodeposition current, (c) the polarization curves and (d) the corresponding Tafel plots at different electrodeposition time.

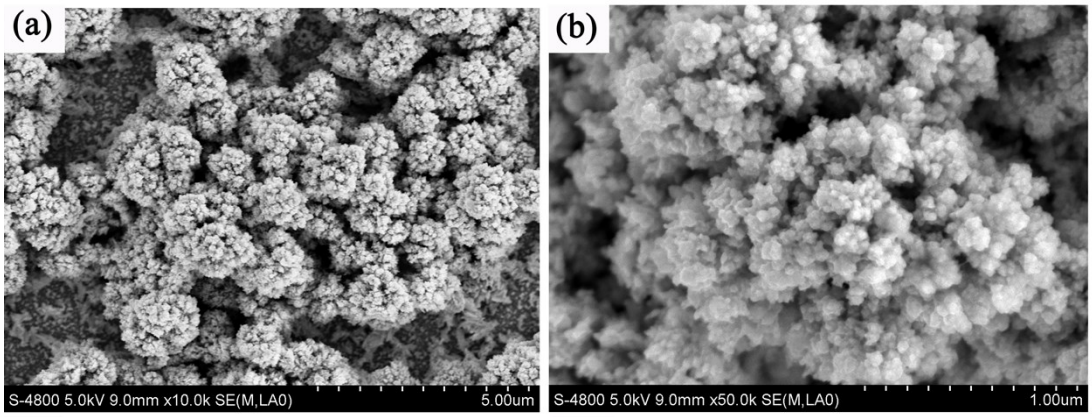

Fig. S7 The SEM images (a) and (b) of NICC/SSF electrodes after chronoamperometry test for HER.

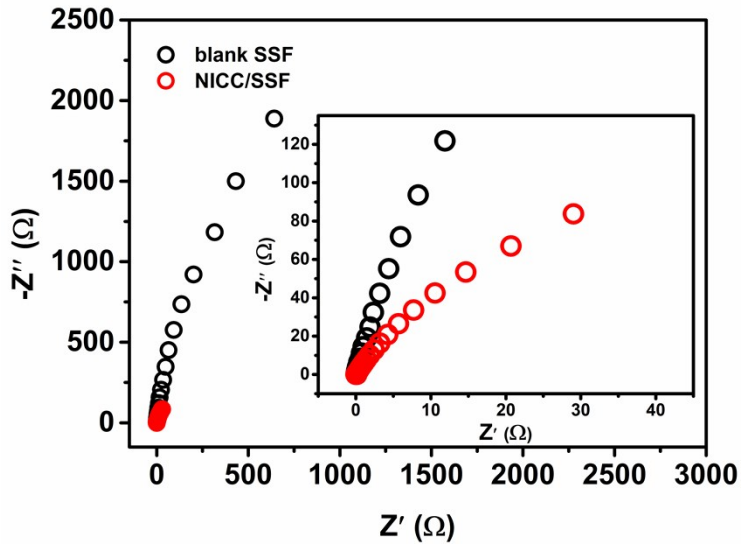

Fig. S8 The EIS at 1.52 V vs. RHE of the blank SSF and NICC/SSF electrodes in 1 M KOH.

The alternating-current impedance of NICC/SSF electrode is less than that of the blank SSF, which indicates its favourable electron transport efficiency during the OER process. The nickel-ferrochrome compound on the SSF could drastically improve the conductivity of NICC/SSF electrode. Moreover, the characteristic 3D architecture is in favour of forming an efficient transport channel during the catalytic process. Therefore, NICC/SSF showed low resistance and high electron transport efficiency.

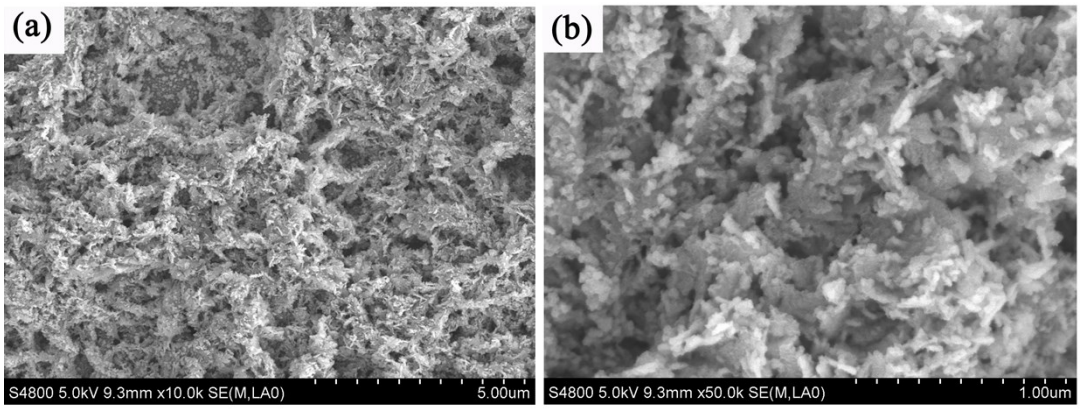

Fig. S9 The SEM images (a) and (b) of NICC/SSF electrodes after chronoamperometry test for OER.

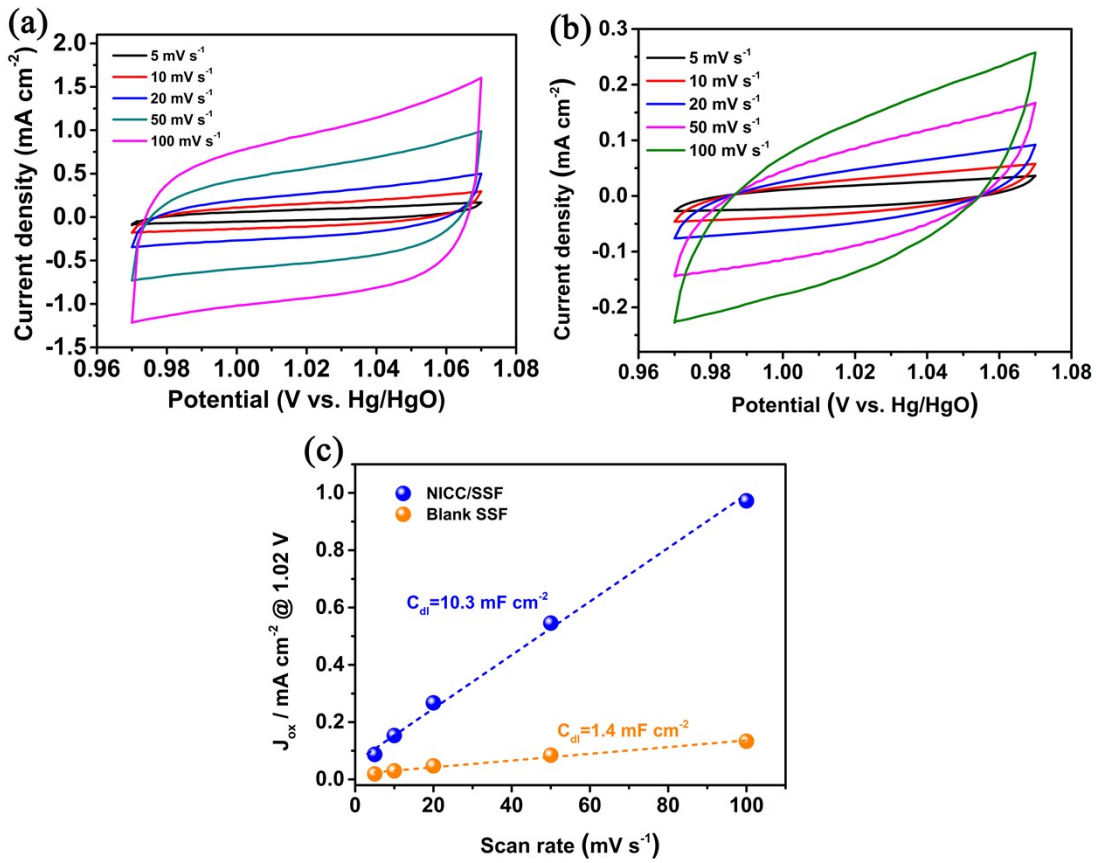

Fig. S10 Typical CV curves of NICC/SSF (a) and blank SSF (b) with scan rates ranging from 5 mV s^{-1} to 100 mV s^{-1} and the scanning potential range is from 0.97 V to 1.07 V; (c) linear fitting of the oxidation currents of the catalysts at 1.02 V vs. RHE versus scan rates.

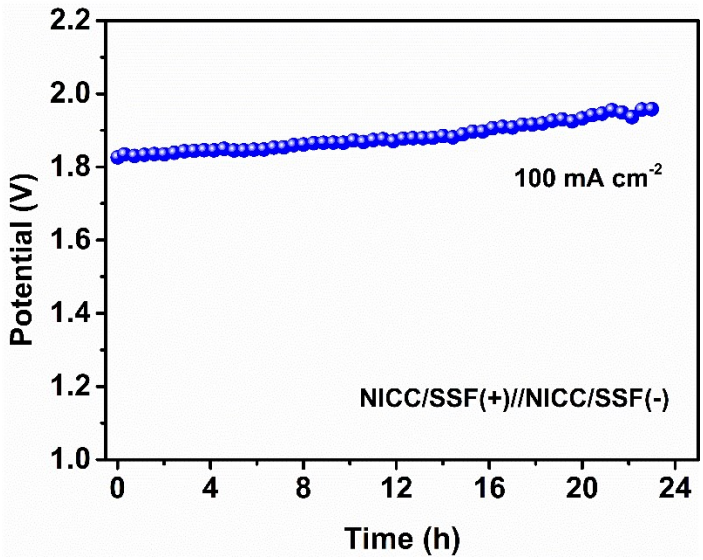

Fig. S11 Long-term stability test of NICC/SSF as both anode and cathode at a constant current density of 100 mA cm^{-2} in 1 M KOH;

Table S2. Comparison of HER performances in 1.0 M KOH for NICC/SSF with other catalysts.

Catalysts	Current denstity (j, mA cm^{-2})	Overpotential at the correspondin g j (mV)	Tafel slope (mV dec^{-1})	References
$Ni_{1.5}Co_{0.5}$@ N-C NT/NF	10	114	117	1
CuO@Ni/NiFe hydroxide	10	125	86	2
Porous Ni-Cr-Fe alloy	/	/	130	3
$CoNiS_x$/NF-25	10	123	89	4
Co-NCNTFs//NF	10	141		5
NiO nanorod arrays	10	110	100	6
P-substituted $CoSe_2$	10	92	90	7
core-shell $CuCo_2S_4$/$NiCo_2S_4$	10	206	90	8
Co_3O_4@Ni	10	130	53	9
porous $CuCo_2O_4$ nanosheet	10	115	153	10
Sandwich-like $NiSe_2$/Ni_2P@FeP	10	113	73.1	11
NICC/SSF	10/20	85/112	85	This work
Pt/C	10/20	53/72	78	This work

Table S3. Comparisons of the various OER catalysts in alkaline electrolyte according to the reports and this paper.

Catalysts	Current denstity (j, mA cm^{-2})	Overpotential at the corresponding j (mV)	Tafel slope (mV dec^{-1})	References
trimetallic NiFeCr LDH	10	280	130	12
Ni-Fe LDH hollow nanoprisms	10	280	49.4	13
NiFeCr-LDHs/g-C_3N_4)	10	223	89	14
Fe–$NiCr_2O_4$/NF	20	228	57	15
Porous Ni_8Fe_2 alloy	10	269	42.5	16
NiOOH-decorated α-FeOOH nanosheet array (ASF)	10	256	45	17
$NiCo_2O_4$@C@NF	10	242	86	18
ZnFeCo LDH	10	221	58.7	19
CoNG/Ru nanocomposites	10	350	82.3	20
O-incorporated CoP	10	310	83.5	21
$CoFe_2O_4$/C NRAs	10	240	45	22
core-shell $CuCo_2S_4$/$NiCo_2S_4$	10	270	57	23
NiCoP/C nanoboxes	10	330	96	24
NiMn LDH	10	350	40	25
α-$Co_4Fe(OH)_x$ nanosheets	10	295	52	26
NICC/SSF	10	274	42	This work
RuO_2/SSF	10	305	58	This work

Table S4. Comparisons of different bifunctional electrocatalysts for overall water splitting in 1.0 M KOH solution.

Catalysts	Current denstity (j, mA cm^{-2})	Cell voltage (V)	References
$Co(OH)_2$@NCNTs	10	1.72	27
$Co_5Mo_{1.0}O$ NSs//$Co_5Mo_{1.0}P$ NSs	10	1.68	28
N-$NiCo_2O_4$@C@NF	10	1.67	29
SSFS	10	1.64	30
NiFe LDH@NiCoP	10	1.57	31
CoFe Oxyhydroxide NSs	10	1.64	32
P-Co_3O_4 NWs	10	1.63	33
NICC/SSF	10/20	1.60/1.67	This work

References

[1] T. F. Li, S. L. Li, Q. Y. Liu, J. W. Yin, D. M. Sun, M. Y. Zhang, L. Xu, Y. W. Tang and Y. W. Zhang, *Adv. Sci.,* 2020, **7**, 1902371.

[2] Y. H. Liu, Z. Y. Jin, X. Q. Tian, X. Q. Li, Q. Zhao and D. Xiao, *Electrochim. Acta,* 2019, **318**, 695-702.

[3] Y. F. Xiao, Y. Liu, Z. Tang, L. Wu, Y. Zeng, Y. F. Xua and Y. H. He, *RSC Adv.,* 2016, **6**, 51096-51105.

[4] W. T. Lu, X. W. Li, F. Wei, K. Cheng, W. H. Li, Y. H. Zhou, W. Q. Zheng, L. Pan and G. Zhang, *ACS Sustainable Chem. Eng.,* 2019, **7**, 12501-12509.

[5] Q. Y. Yuan, Y. X. Yu, Y. J. Gong and X. F. Bi, *ACS Appl. Mater. Interfaces,* 2020, **12**, 3592-3602.

[6] T. Zhang, M. Y. Wu, D. Y. Yan, J. Mao, H. Liu, W. B. Hu, X. W. Du, T. Ling and S. Z. Qiao, *Nano Energy,* 2018, **43**, 103-109.

[7] Y. P. Zhu, H. C. Chen, C. S. Hsu, T. S. Lin, C. J. Chang, S. C. Chang, L. D. Tsai and H. M. Chen, *ACS Energy Lett.,* 2019, **4**, 987-994.

[8] L. Ma, J. W. Liang, T. Chen, Y. J. Liu, S. Z. Li and G. J. Fang, *Electrochim. Acta,* 2019, **326**, 135002.

[9] R. C. Li, D. Zhou, J. X. Luo, W. M. Xu, J. W. Li, S. W. Li, P. P. Cheng and D. S. Yuan, *J. Power Sources,* 2017, **341**, 250-256.

[10] A. T. A. Ahmed, S. M. Pawar, A. I. Inamdar, H. Kim and H. Im, *Adv. Mater. Interfaces,* 2020, **7**, 1901515.

[11] J. H. Lin, H. H. Wang, Y. T. Yan, J. Cao, C. Q. Qu, X. H. Zheng, J. C. Feng and J. L. Qi, *J. Power Sources,* 2020, **445**, 227294.

[12] Y. Yang, L. N. Dang, M. J. Shearer, H. Y. Sheng, W. J Li, J. Chen, P. Xiao, Y. H. Zhang, R. J. Hamers and S. Jin, *Adv. Energy Mater.,* 2018, **8**, 1703189.

[13] L. Yu, J. F. Yang, B. Y. Guan, Y. Lu and X. W. (David) Lou, *Angew. Chem. Int. Ed.,* 2018, **57**, 172-176.

[14] G. Chen, J. Liu, Y. li, P. Anand, W. Wu, Y. Chen and C. L. Xu, *Nanotechnology,* 2019, **30**, 494001.

[15] J. X. Zhao, X. H. Li, G. W. Cui and X. P. Sun, *Chem. Commun.,* 2018, **54**, 5462-5465.

[16] W. B. Li, Q. F. Hu, Y. W. Liu, M. M. Zhang, J. J. Wang, X. P. Han, C. Zhong, W. B. Hu and Y. D. Deng, *J. Mater. Sci. Technol.,* 2020, **37**, 154-160.

[17] D. B. Zhang, X. G. Kong, M. H. Jiang, D. Q. Lei and X. D. Lei, *ACS Sustainable Chem. Eng.,* 2019, **7**, 4420-4428.

[18] Y. Ha, L. X. Shi, X. X. Yan, Z. L. Chen, Y. P. Li, W. Xu and R. B. Wu, *ACS Appl. Mater. Interfaces,* 2019, **11**, 45546-45553.

[19] J. X. Han, J. Zhang, T. T. Wang, Q. Xiong, W. Wang, L. X. Cao and B. H. Dong, *ACS Sustainable Chem. Eng.,* 2019, **7**, 13105-13114.

[20] T. He, Y. Peng, Q. X. Li, J. E. Lu, Q. M. Liu, R. Mercado, Y. Chen, F. Nichols, Y. Zhang and S. W. Chen, *ACS Appl. Mater. Interfaces,* 2019, **11**, 46912-46919.

[21] G. Y. Zhou, M. Li, Y. L. Li, H. Dong, D. M. Sun, X. E. Liu, L. Xu, Z. Q. Tian and Y. W. Tang, *Adv. Funct. Mater.,* 2020, **30**, 1905252.

[22] X. F. Lu, L. F. Gu, J. W. Wang, W. J. Wu, P. Q. Liao and G. R. Li, *Adv. Mater.,* 2017, **29**, 1604437.

[23] L. Ma, J. W. Liang, T. Chen, Y. J. Liu, S. Z. Li and G. J. Fang, *Electrochim. Acta,* 2019, **326**, 135002.

[24] P. L. He, X. Y. Yu and X. W. Lou, *Angew. Chem. Int. Ed.,* 2017, **56**, 3897-3900.

[25] A. Sumboja, J. W. Chen, Y. Zong, P. S. Lee and Z. L. Liu, *Nanoscale,* 2017, **9**, 774-780.

[26] H. Y. Jin, S. J. Mao, G. P. Zhan, F. Xu, X. B. Bao and Y. Wang, *J. Mater. Chem. A,* 2017, **5**, 1078-1084.

[27] P. Guo, J. Wu, X. B. Li, J. Luo, W. M. Lau, H. Liu and X. L. Sun, *Nano Energy,* 2018, **47**, 96-104.

[28] Y. Zhang, Q. Shao, S. Long and X. Huang, *Nano Energy,* 2018, **45**, 448-55.

[29] Y. Ha, L. X. Shi, X. X. Yan, Z. L. Chen, Y. P. Li, W. Xu and R. B. Wu, *ACS Appl. Mater. Interfaces,* 2019, **11**, 45546-45553.

[30] X. Liu, B. You and Y. J. Sun, *ACS Sustainable Chem. Eng.,* 2017, **5**, 4778-4784.

[31] P. Babar, A. Lokhande, H. H. Shin, B. Pawar, M. G. Gang and S. Pawar, *Small,* 2018, **14**, 1702568.

[32] H. J. Zhang, X. P. Li, A. Hähnel, V. Naumann, C. Lin, S. Azimi, S. L. Schweizer, A. W. Maijenburg and R. B. Wehrspohn, *Adv. Funct. Mater.,* 2018, **28**, 1706847.

[33] Z. Wang, H. Liu, R. Ge, X. Ren, J. Ren, D. Yang, L. Zhang and X. Sun, *ACS Catalysis,* 2018, **8**,

2236-2241.